

E. R. Gray, E. L. Hubbard,* F. E. Mills, C. W. Owen
R. E. Peters, A. G. Ruggiero and M. F. Shea
Fermi National Accelerator Laboratory**
Batavia, Illinois

Summary

Measurements are presented of the transverse properties of the booster synchrotron. The principal transverse limitations to operational performance have been due to restricted aperture and improper multiturn injection. In addition to these features, working point, chromaticities, high-intensity effects, and injection matching are discussed.

The 200-MeV Line

Over the past year, a number of hardware changes have been made to improve the operation of the 200-MeV transport system. These improvements include new power-supply controllers, new readback circuits, and new forty eight channel wire profile monitors.

A major change in the injection line design was made last spring. Two quadrupole magnets were moved to accommodate a debuncher cavity. Four quadrupole magnets were added to the horizontal translation near the injection point to make this translation achromatic and provide beam matching at injection.

The result of all this work has been improved reliability and predictability of the transport system. Operation of the line with both the horizontal and vertical translations nearly achromatic has brought about improved stability. The line will transmit a momentum width greater than 0.4%, which is necessary for optimal debuncher operation. Separation of the steering and focussing properties of the line has allowed independent optimization of the injection angle, position, and beam width. With a nominal matched vertical beam height of 3 cm, the horizontal width can be as small as .6 cm for multiturn injection. Presently, the horizontal width is approximately 2 cm for two-turn injection.

Multiturn Injection

Injection into the booster is accomplished with an orbit-bump system that is local to the injection straight section. The orbit-bump magnets, magnetic septum, and electrostatic wire septum allow radial phase-space stacking. The orbital bump power supply provides a maximum radial orbit excursion of 48 mm.¹ The current waveform is a half-sine-wave whose length can be varied from 74 to 160 μ sec. At minimum pulse length and maximum excitation, the orbit decay at beam time is 5.2 mm per turn.

* Presently at Gulf General Atomic, LaJolla, California.

** Operated by Universities Research Association, Inc. under contract with the U. S. Energy Research and Development Administration.

Any relative misalignment among the injected beam direction, electrostatic inflector orientation, and closed-orbit direction will increase the effective septum thickness and cause dilution of the radial phase plane. A measurement of effective septum thickness can be made by the following means. Both the injected beam and the closed orbit are translated until heavy scraping is observed on both sides of the septum. A single wire is stepped through the beam and its current output is digitized with a fast storage device. A computer program is then used to reduce the data to a time sequence of beam profiles, as shown in Figure 1.² These data were obtained while operating at a radial tune of 6.5 and injecting a fraction of a turn.

The first set of profiles in the lower left of the figure is of the scraped injected beam. The next set shows the beam scraping on the inside of the septum (2.6 cm) after the first revolution. The narrow area between the first two profile sets is the apparent septum thickness, which is less than 1 mm. The return of the beam on the second, third, and fourth revolutions is also seen. The movement of later revolutions toward the right is due to the decay of the orbit bump.

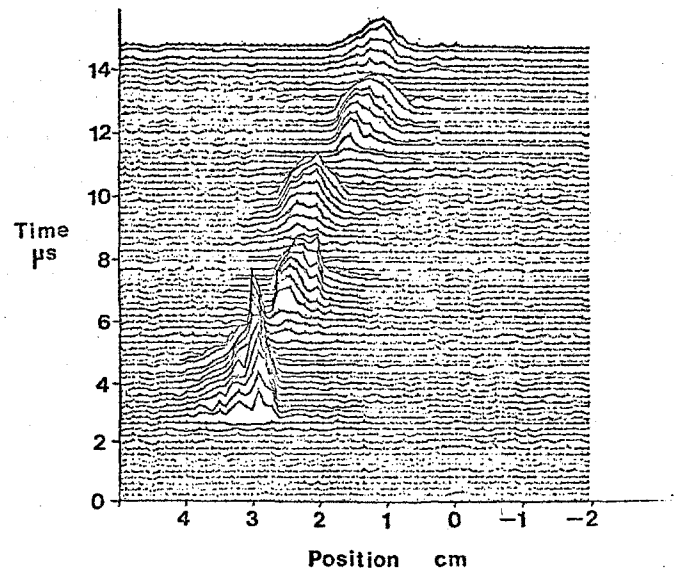


Figure 1. Motion of the beam position during multiturn injection.

The restricted aperture (see below) of the booster places a limitation on the performance of the multiturn injection system. As a consequence, in typical operation, two turns are injected. Higher density phase-space filling can be achieved by reducing the orbit-bump decay rate and injecting over a longer period of time. It is possible to inject into the booster in this manner, but the results are degraded by the time dependence of the injected momentum due to the transient phase shift of the debuncher.³ As the aperture of the booster is

increased, it may be possible to employ the half-integral injection scheme originally contemplated, although this leads to a less dense phase-space filling.

Beta-Function and Aperture Measurements

Each period of the booster lattice contains two sets of (direct current) air-core trim elements located near the beta-function maxima. Each group consists of a radial dipole, vertical dipole, quadrupole, and a skew quadrupole.

The radial and vertical beta functions have been determined at each trim quadrupole location. This was done by measuring the tune as a function of the strength of a single trim quadrupole. A typical curve, obtained at a radial (vertical) beta maximum (beta minimum) is shown in Figure 2. The beta function is proportional to the slope of the curve. Although the procedure is quite simple, the expected vertical tune variation (Figure 2) is only 0.008. Consequently, a very careful determination of the tune is required. The average results obtained at the beta-maximum locations are within 3% of design values, with root-mean-square azimuthal variations of 10%. At the beta-minimum locations, where the measurements are less precise, the results are within 7% of the design values with root-mean-square azimuthal variations of 10% in the horizontal plane and 22% in the vertical plane. The relatively large vertical beta-minimum fluctuations are not believed to be the source of any aperture restrictions.

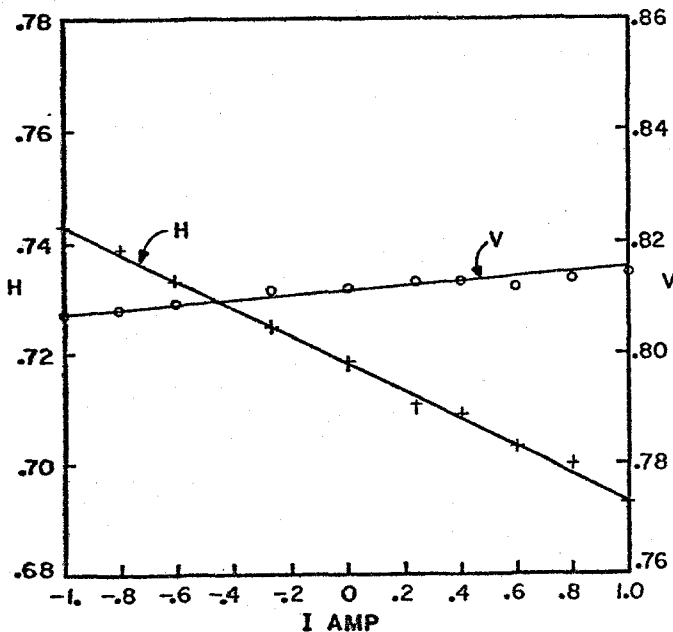


Figure 2. Radial and vertical tune versus excitation strength of a single trim quadrupole.

These data imply a radial half integer stop-band width of about 0.04. This is in good agreement with independent measurements of the stop-band width.

Local aperture widths have been determined by fixing the relative strengths of three consecutive (beta maximum) dipoles to generate an orbit perturbation. In the 21 radial beta-maximum locations where the measurement can be performed, the upper limit of

the aperture width for 95% beam loss is 90 mm ($\beta = 33.66$). If all straight sections had this width, the machine acceptance would be 60π mm-mrad. The useful vertical acceptance is limited by the amount of aperture required for the proper location of the extraction septum. At the present time, the vertical acceptance is 10.5π mm-mrad. Once the new septum magnet is installed, the vertical acceptance will be 20π mm-mrad. The remainder of the ring has a vertical aperture corresponding to an acceptance of 33π mm-mrad (design is 40π mm-mrad).

Dynamical Tune

Both vertical and horizontal tunes have been measured as a function of time and radius in the booster. The radius was changed with an rf bump, and coherent oscillations were detected after exciting the beam with a fast kicker. The locus of the working point during acceleration is shown under different conditions in Figures 3 and 4. Figure 3 is the result of careless tuning, as evidenced by the crossing of several higher order resonances. By adjusting the radial chromaticity, radial position, and the initial tunes, conditions are obtained as shown in Figure 4. The overall transmission is slightly improved by avoiding the higher order resonances. Under normal operating conditions, the tune is not as well controlled as in Figure 4, but is usually within the triangular region bounded by $3\nu_x = 20$, $2\nu_y - \nu_x = 7$ and $\nu_x + 3\nu_y = 27$.

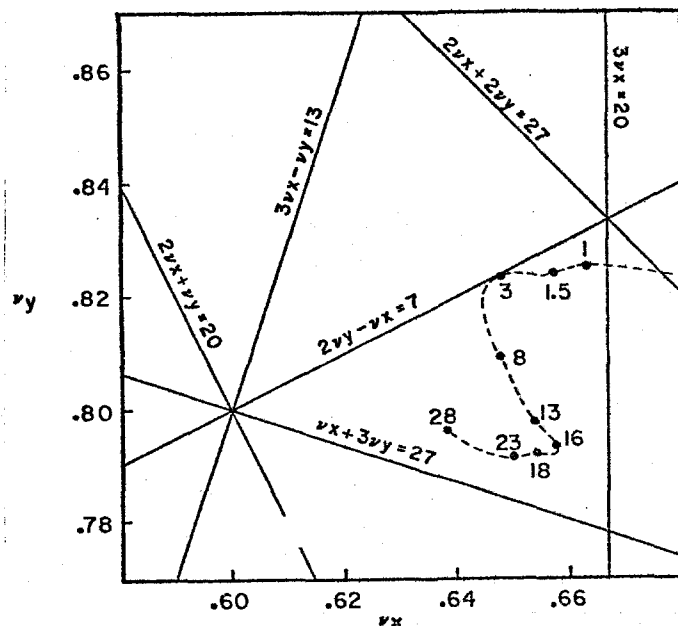


Figure 3. Locus of the working point. The figures on the curve are the measurement times (msec).

Two sets of sextupoles have been installed in the booster. One set is installed in three long straight sections (vertical β -max) 120° apart. These sextupoles are programmed with a two-level current waveform. The level is initially set to adjust the vertical chromaticity at injection and then ramped to a higher value in order to control the head-tail instability near transition. The second set is made of elements installed in each short straight section (horizontal

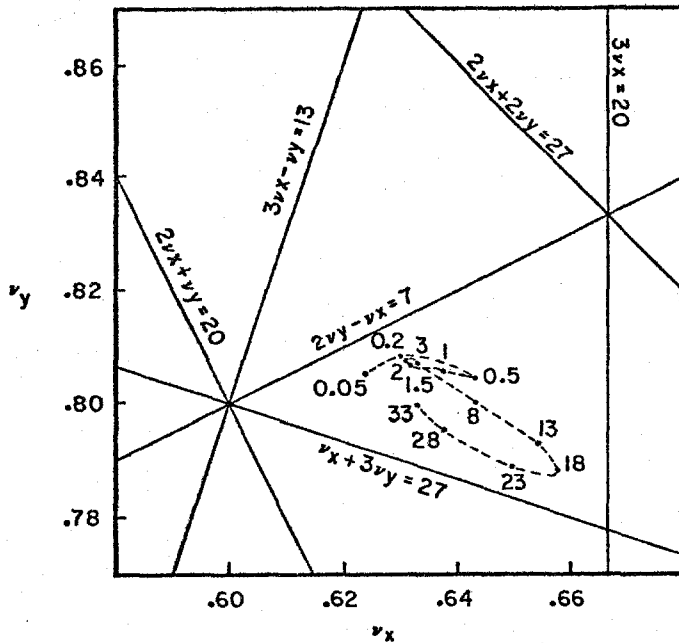


Figure 4. Corrected locus of the working point. The figures on the curve are the measurement times (msec).

β -max) and is used to adjust the radial chromaticity at injection.

Vertical and horizontal chromaticities have been measured with typical sextupole settings. The vertical chromaticity ($\Delta\nu/\nu/\Delta p/p$) is 0.4 at 5 msec, -0.1 at 16 msec and 0.24 at 28 msec. The horizontal chromaticity is -1.6 at 5 msec, but at later times the horizontal tune has a more complicated dependence on radius. The data shown in Figure 5 illustrate this behavior.

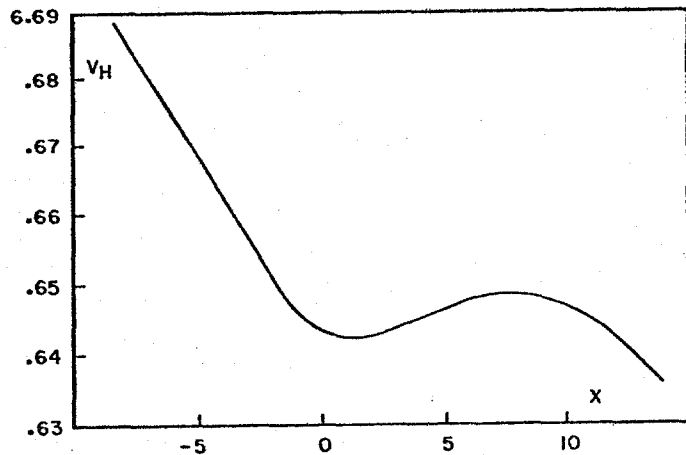


Figure 5. Radial tune versus radial position ($X_p = 1.84\text{m}$) at 25 msec.

High Intensity Effects

The Laslett coherent tune shift, $\Delta\nu$, has been measured versus intensity and beam energy during a typical acceleration cycle. Tunes were measured at injection by detecting spontaneous coherent oscillations during the first 100 μsec . Vertical tune measurements at 8 msec and 18 msec after injection were made by exciting the beam with a fast kicker.

The beam intensity was varied by generating a transverse phase-space mismatch at injection so that the aperture was always filled. The beam charge was detected a few turns after the tune was measured.

The Laslett coherent tune shift is given by the formula⁴

$$\Delta\nu = \frac{-Nr_p R}{\pi\nu\gamma} \left[(\alpha_M + \alpha_E) + \frac{\alpha_E}{B\beta^2\gamma^2} \right]$$

where B is the bunching factor, N the number of protons per turn, r_p the classical proton radius and α_E , α_M are related to the Laslett image coefficients.

Table I summarizes parameters, calculations and measurements of the vertical tune shift. The data show that the shift is linear with the intensity, and the vertical shift is much larger than the radial.

Table I

Tune-Shift Measurements and Calculations
for $N = 1.0 \times 10^{12}$

Time	Injection	8 msec	18 msec
β	0.5662	0.8839	0.9843
γ	1.2132	2.14	5.66
B	0.5, 1.0	0.2	0.1
ν	--	6.8	--
$\Delta\nu_{\text{meas}}$	-0.022	-0.010	-0.005
$\Delta\nu_{\text{meas}}$	-0.017	--	--
$\Delta\nu_{\text{error}}$	--	± 0.0015	--
α_M	--	0.218/cm ²	--
α_E	--	0.0519/cm ²	--
$\Delta\nu_{\text{calc}}$	--	-0.0081	-0.0027

α_M and α_E have been calculated from measurements at injection, once with bunched beam ($B = 0.5$) and then with unbunched beam ($B = 1$). These values were then used to predict the higher energy tune shifts. The overall agreement between the measured and predicted tune shifts is satisfactory.

The only instability so far observed in the booster is a coherent vertical oscillation which is believed to be enhanced by the head-tail effect. The circumstances under which the head-tail effect occurs in the booster have already been described in the literature.⁵ At the present peak intensity ($\approx 150\text{ mA}$) the onset of the beam instability occurs about 10 msec before transition, much earlier than at lower intensity. It can be controlled with the long straight sextupoles, but the present two-level excitation will probably be inadequate at higher intensities.

References

1. R. Winje, "A 230-kJ Pulsed Power Supply," to be published, proceedings of this conference.

2. M. Shea, "Interaction of Accelerator Controls and Diagnostics," to be published, proceedings of this conference.
3. C. W. Owen, et al., "A 200-MHz Debuncher for the Fermilab Injector," to be published, proceedings of this conference.
4. J. Laslett, "On Intensity Limitations Imposed by Transverse Space Charge Effects in Circular Particle Accelerators," Proceedings of the 1963 Summer Study on Storage Rings, Accelerators and Experimentation at Super High Energies, Brookhaven, p. 325.
5. E. L. Hubbard, et al., "Correction of Intensity Dependent Beam Loss in the NAL Booster Synchrotron," IEEE Trans. on Nucl. Sci., NS-20, No. 3, p. 863, (1973).